HHS Public Access

Author manuscript

Chem Commun (Camb). Author manuscript; available in PMC 2020 January 17.

Published in final edited form as:

Chem Commun (Camb). 2019 January 17; 55(7): 913–916. doi:10.1039/c8cc08453j.

The Hydrogen Atom Transfer Reactivity of a Porphyrinoid Cobalt Superoxide Complex

Jireh Joy D. Sacramento and **David P. Goldberg**

Department of Chemistry, The Johns Hopkins University, 3400 N. Charles Street, Baltimore, MD 21218, USA. dpg@jhu.edu

Abstract

The H-atom transfer (HAT) reactivity of a corrolazine cobalt superoxide with weak O–H and N–H substrates has been demonstrated. Kinetic analysis shows relatively fast rates of HAT with diphenylhydrazine (DPH). A kinetic isotope effect (KIE) and Eyring activation parameters are consistent with an HAT mechanism.

Table of Contents

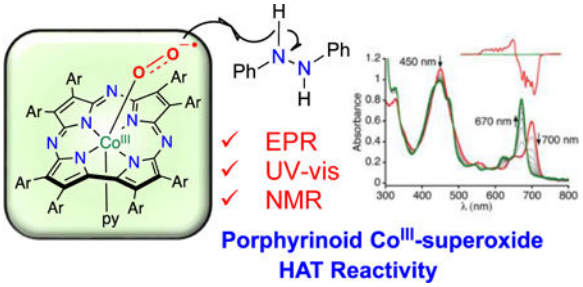

The H-atom transfer reactivity of a porphyrinoid cobalt superoxide with weak O-H and N-H substrates has been demonstrated.

The activation of dioxygen at both heme and nonheme metal sites in biology is the first step in a wide range of substrate oxidation reactions.[1] The binding of O_2 at a transition metal center (M^{n+}) typically involves one electron transfer from the metal to the bound O_2 molecule, giving a metal-superoxide species ($M^{n+1}(O_2^{\bullet-})$). The controlled addition of electrons and protons may eventually result in O–O cleavage, giving a high-valent metal-oxo species that reacts via oxidation with substrates of interest. However, the initial $M^{n+1}(O_2^{\bullet-})$ intermediate in certain systems may be responsible for direct attack of the substrate, obviating the need for multielectron/proton transfer prior to substrate oxidation. For example, mechanistic proposals for an intriguing class of heme dioxygenases (tryptophan dioxygenase (TDO), 2,3-indoleamine dioxygenase (IDO)), involve substrate dioxygenation beginning with the direct attack of the indole substrate by the superoxo adduct $Fe^{III}(O_2^{\bullet-})$(porphyrin)(His).[2] Similarly, current proposals for the heme enzyme nitric oxide synthase (NOS) suggest a superoxo or peroxo-iron species initiates the attack on an N-hydroxy-L-

---

†Electronic Supplementary Information (ESI) available: Experimental details. See DOI: 10.1039/x0xx00000x

arginine substrate, ultimately producing L-citrulline and NO products.[3] An iron(III)-superoxo intermediate in nonheme iron enzymes, including cysteine dioxygenase,[4] myo-inositol oxygenase,[5] and isopenicillin-N-synthase,[6] are also postulated to be active oxidants that carry out direct attack on substrate.

Synthetic metalloporphyrin complexes were shown to reversibly bind dioxygen via metastable metal-superoxide complexes since the early 1970s.[7] More recent elaboration of the porphyrin scaffold has provided access to O_2-derived $Fe^{III}(O_2^{\bullet-})$ species which can be converted into ferric-peroxide and ferric-hydroperoxide species under controlled conditions.[8] The related cobalt porphyrins and phthalocyanines are also known to reversibly bind O_2.[9] However, little is known about the reactivity of these $M^{n+1}(O_2^{\bullet-})$ porphyrinoid species in terms of the direct oxidation of organic substrates.[10] Well-defined nonheme metal-superoxide complexes are also known, but their reactivity toward organic substrates is also poorly understood. It was not until recently that a well-defined, nonheme, cobalt(III)-superoxide was shown to mediate H-atom abstraction from an organic substrate.[11] To our knowledge, there are as of yet no reports on the analogous cobalt-superoxide reactivity in a porphyrinoid system. Herein we describe a $Co^{III}(O_2^{\bullet-})$ porphyrinoid complex that abstracts H-atoms from activated O–H and N–H bond substrates.

The formation of a cobalt(III)-superoxide species with the octa-(4-*tert*-butylphenyl)corrolazine) (TBP_8Cz) ligand was reported previously.[12] The $[Co^{III}(py)(O_2)(TBP_8Cz)]^-$ species (py = pyridine) was prepared via addition of excess dioxygen to $[Co^{II}(py)(TBP_8Cz)]^-$ at low temperature. The superoxide complex was characterized by EPR spectroscopy, giving a spectrum similar to other cobalt(III)-superoxides.[9b, 9d] However, no other spectroscopic characterization was obtained. Herein we provide new low-temperature UV-vis and ^1H NMR spectroscopy on the $[Co^{III}(py)(O_2)(TBP_8Cz)]^-$ complex, as well as on the related Co^{II} and $Co^{III}(py)_2$ complexes. The spectroscopic data fully support the structural assignments of these complexes. These low-temperature spectroscopic methods also provide a means to monitor the reactivity of the superoxo species with organic substrates. It is shown that $[Co^{III}(py)(O_2)(TBP_8Cz)]^-$ is capable of abstracting H-atoms from certain N–H donors, and kinetic studies provide insight into the mechanism of H-atom transfer (HAT).

Reduction of CoIII(py)2(TBP8Cz) to the 5-coordinate anionic [CoII(py)(TBP8Cz)]- was carried out previously by addition of excess NaBH4 in EtOH/py.12 Other reductant/solvent combinations were tested to determine an optimal protocol for the reduction. Addition of $Cr(\eta^6\text{-}C_6H_6)2$, $Co(\eta^5\text{-}(C_5(CH_3)5)2$ or $Bu_4N^+BH_4$- led to the stoichiometric reduction of the CoIII complex to give $[Co^{II}(py)(TBP_8Cz)]$-. The UV-visible spectrum for $Co^{III}(py)2(TBP_8Cz)$ in CH_2Cl_2/pyridine 99/1 (v/v) (445, 543, 622, 670 nm) is converted to a new spectrum with loss of the 670 nm Q-band and growth of new peaks at 612 and 764 nm (Figure S1). The reductant Bu4N+BH4- was found to be the most robust and economical, and therefore was employed for all other studies.

Cooling the Co^{II} complex to −65 °C leads to no significant changes in the UV-vis spectrum. However, addition of excess O_2 at this temperature causes the immediate disappearance of the spectral signature for the Co^{II} complex, and the appearance of a new spectrum with λ_{max} = 450, 600, and 700 nm, as shown in Figure 1. The new spectrum is assigned to the Co-

dioxygen adduct $[Co^{III}(py)(O_2)(TBP_8Cz)]^-$. This species is stable for > 5 h at temperatures equal to or lower than −65 °C. However, the Co(III)-superoxo complex slowly converts to the $Co^{III}(py)_2$ species upon warming above −65 °C, as evidenced by a decrease of the 700 nm peak and a concomitant growth of a peak at 670 nm characteristic of $Co^{III}(py)_2(TBP_8Cz)$. Reversible binding of O_2 is noted if the solution is sparged with Ar(g) for 20 min at −65 °C, which causes a return of the Co^{II} absorbance spectrum. Further addition of excess O_2 regenerates the spectrum for the superoxo species (Figure S2). The generation of the superoxo complex is summarized in Scheme 1.

The EPR spectrum of the Co^{II} complex (Figure S3) matches that previously reported for $[Co^{II}(py)(TBP_8Cz)]^-$ generated in a different solvent system with a different reductant.[12] The EPR spectra of $Co^{III}(O_2^-)$ complexes are well-documented and follow a characteristic pattern.[9b, 9d] The spectrum of $[Co^{III}(py)(O_2)(TBP_8Cz)]^-$ (Figure 1 inset, red line) follows this pattern and matches what was reported previously.[12] The NMR spectra for the three cobalt species are shown in Figure 2. The bis(pyridine) complex $Co^{III}(py)_2(TBP_8Cz)$ exhibits a diamagnetic ^1H NMR spectrum, as expected for a low-spin d^6 ion. Upon reduction to the Co^{II} species, a paramagnetic spectrum appears, consistent with a low-spin d^7 ($S = ½$) complex. Addition of O_2 causes the ^1H NMR spectrum of the Co^{II} complex to disappear and be replaced by a spectrum with broadened, poorly defined peaks. This spectrum is consistent with the presence of a paramagnetic superoxo species with spin delocalization over the Co and O_2 moieties. The spectrum for Co^{II} is regenerated upon sparging with $Ar_{(g)}$, as also seen in the UV-vis data. Taken together, the EPR and NMR data confirm that the reduced Co^{II} complex is quantitatively converted into the cobalt(III)-superoxo complex, $[Co^{III}(py)(O_2)(TBP_8Cz)]^-$.

The reactivity of $[Co^{III}(py)(O_2)(TBP_8Cz)]^-$ with H-atom donors was examined. Initial experiments were focused on determining if the superoxo complex could oxidize C–H substrates. We began with potential H-atom donors with relatively weak C–H bonds, such as dihydroanthracene (BDE(C–H) = 80.6 kcal/mol)[13] or xanthene (BDE(C–H) = 77.9 kcal/mol).[13] Addition of an excess of C-H substrate (25 – 100 equiv) to the superoxo complex in CH_2Cl_2/py at −65 °C resulted in no spectroscopic change by UV-vis over 2 h, indicating that the $Co^{III}(O_2^{\bullet-})$ species was unreactive toward these C-H substrates. However, reaction of O–H and N–H substrates led to different results. Addition of excess TEMPOH under the same conditions led to the isosbestic conversion of the superoxo complex to $Co^{III}(py)_2(TBP_8Cz)$ (Figure S5). The production of the bis(pyridine)-ligated complex was consistent with an initial H-atom transfer (HAT) from TEMPOH to give a cobalt(III)-hydroperoxo complex, that rapidly loses hydroperoxide via displacement by the excess pyridine. The stability of the low-spin, d^6 $Co^{III}(py)_2$ unit, as evidenced by the high formation constant for pyridine ($\beta_2 = 9.0 \times 10^7\ M^{-2}$) measured in CH_2Cl_2,[14] likely provides much of the driving force for the second step.

Given that TEMPOH has a BDE(O-H) of 72.1 kcal/mol,[13] we examined N-H substrates of similar strength. Both phenylhydrazine (BDE(N–H) = 75.0 kcal/mol) and diphenylhydrazine (DPH) (BDE(N–H) = 71.7 kcal/mol)[13] react with the superoxide complex at −65 °C, as seen by the same spectral changes in the UV-vis that were seen for the reaction with TEMPOH. The isosbestic conversion of $[Co^{III}(py)(O_2)(TBP_8Cz)]^-$ to $Co^{III}(py)_2(TBP_8Cz)$ for the

reaction with DPH is shown in Figure 3. The absorbance at 670 nm ($\varepsilon = 5.3 \times 10^4$ M^{-1} cm^{-1}) indicates an 80% yield of the final bis(pyridine) product. A complete loss of the EPR signal from the superoxide complex was also noted. The final EPR-silent species can be assigned to the low-spin $Co^{III}(py)_2(TBP_8Cz)$ complex.

If the DPH reaction involves HAT to the superoxide complex, it should lead to formation of azobenzene, which is the result of a formal dehydrogenation (i.e. two HAT events) of the substrate. Carrying out the reaction of $[Co^{III}(py)(O_2)(TBP_8Cz)]^-$ with excess DPH in CD_2Cl_2/py-d_5 (20/1) at −65 °C led to identification of both azobenzene and the diamagnetic $Co^{III}(py)_2(TBP_8Cz)$ by ^1H NMR spectroscopy (Figure S7). The reaction stoichiometry is $[Co^{III}(py)(O_2)(TBP_8Cz)]^-$:DPH 2:1, assuming a single superoxide complex accepts only one hydrogen atom (Scheme 2). A comparison of the integrated areas for the ^1H NMR peaks corresponding to azobenzene versus the Co^{III} product confirmed the expected 2:1 stoichiometry. Similarly, comparison of integrations with the peak for an internal standard (3,5-dimethylanisole) gave a yield of 93 ± 12% for azobenzene, and 87 ± 12% for $Co^{III}(py)_2(TBP_8Cz)$.

A proposed mechanism for the observed reactions between H-atom donors and the cobalt-superoxide complex is shown in Scheme 3. The first step involves HAT from the donor to the OOH^- ligand is then displaced in a rapid second step by excess pyridine to give the stable $Co^{III}(py)_2$ species. The isosbestic conversion between the superoxo and bis(pyridine) complexes, and the lack of any spectroscopic (UV-Vis, NMR) evidence for the $Co^{III}(OOH)$ species, support this mechanism. Attempts were made to independently generate the $Co^{III}(OOH)$ species by addition of hydrogen peroxide and triethylamine to $Co^{III}(py)_2(TBP_8Cz)$, but no reaction was observed, and addition of a large excess of H_2O_2/Et_3N led to bleaching of the solution.

To gain further mechanistic insights into the reaction of $[Co^{III}(O_2)(py)(TBP_8Cz)]^-$ with DPH, kinetic analyses were performed. The rate of the reaction with excess DPH (pseudo-first-order conditions) was followed by the disappearance of the 700 nm peak corresponding to the starting material, as well as the growth of the 670 nm peak corresponding to the $Co^{III}(py)_2$ product. First-order behaviour was observed (>5 half-lives) and fitting of the data (FIGURE S8) led to first-order rate constants (K_{OBS}) that were shown to vary linearly with substrate concentration. A second-order rate law was implicated and was consistent with HAT being the rate-determining step, with a $K_2 = 3.6(8)$ M^{-1} s^{-1}.

Additional support for an HAT mechanism comes from the observation of a kinetic isotope effect (KIE). Substitution of deuterium for the N–H protons led to a significant decrease in second-order rate constant (DPH, 3.6(8) M^{-1} s^{-1}; DPH-d_2, 0.39(8) M^{-1} s^{-1}), giving a KIE (k_H/k_D) = 9.2 (Figure 4a). This relatively large KIE provides compelling evidence that the rate determining step involves N-H bond cleavage, as expected for an H-atom transfer.

An Eyring plot for the reaction with DPH constructed from data at −85 °C, −75 °C and −65 °C yielded the activation parameters $\Delta H^{\ddagger} = 6.7 \pm 0.1$ kcal mol^{-1} and $\Delta S^{\ddagger} = -23 \pm 0.4$ cal mol^{-1} K^{-1} (Figure 4b). The relatively large, negative activation entropy is consistent with the bimolecular nature of an HAT reaction and implicates a well-ordered transition state.

The H-atom transfer reactivity of a few other discrete, well-defined $M(O_2^{\bullet-})$ complexes with M = Cu,[15] Cr,[16] Ni,[17] and Fe[18] has been described. The oxidation of weak C-H bonds is quite rare,[18b] but the abstraction of hydrogen from either O–H or N–H bonds with relatively low BDEs (66 – 83 kcal/mol) is more common.[15, 16c, 18a] Interestingly, only two other cobalt-superoxide complexes besides $[Co^{III}(py)(O_2)(TBP_8Cz)]^-$ have been shown to abstract H-atoms from organic substrates, and both involved weak O–H bonds.[11, 19] The latter complexes are derived from nonheme ligand sets. Thus there is limited kinetic information to compare the reactivity of $[Co^{III}(py)(O_2)(TBP_8Cz)]^-$ with other $M(O_2^{\bullet-})$ complexes involved in HAT reactions. In terms of activation parameters, Meyer has shown that a dicopper μ−1,2-superoxide complex reacts with TEMPOH with $\Delta H^{\ddagger} = 9.03 \pm 0.41$ kcal mol $^{-1}$ and $\Delta S^{\ddagger} = -26.8 \pm 2$ cal mol^{-1} K^{-1}, which are similar to those reported here for $[Co^{III}(O_2)(py)(TBP_8Cz)]^-$ and are consistent with a similar HAT mechanism.[15b] The latter study also describes the reactivity of the $Cu_2(\mu{-}1,2\text{-}O_2^{\bullet-})$ complex with the N–H substrate phenylhydrazine (BDE(N-H) = 75.0 kcal mol^{-1}), a close analog of DPH. A second-order rate constant of 0.81 M^{-1} s^{-1} at −20 °C was reported for the oxidation of phenylhydrazine. A rate constant of $k_2 = 89.4$ M^{-1} s^{-1} at the same temperature (−20 °C) is predicted for $[Co^{III}(py)(O_2)(TBP_8Cz)]^-$ via extrapolation from the measured activation parameters, allowing for a direct comparison of the kinetics of N–H cleavage. The second-order rate constants indicate that the cobalt complex is one hundred-fold more reactive than the dicopper superoxo-bridged species in N–H cleavage. The same Cu^{II}_2 complex reacts with the O–H donor TEMPOH, which has a BDE(O–H) (72.1 kcal/mol) close to that of DPH (71.7 kcal/mol), with a rate constant for HAT of $k_2 = 0.13$ M^{-1} s^{-1}, which is seven hundred-fold slower than that seen for $[Co^{III}(py)(O_2)(TBP_8Cz)]^-$ in reaction with DPH. The origins of this differential reactivity (e.g. steric or electronic factors) remain to be determined.

In summary, we have shown that a porphyrinoid cobalt(III)-superoxide complex is competent to abstract hydrogen atoms from relatively weak O–H and N–H bonds. The $Co^{III}(O_2^{\bullet-})$ complex is significantly more reactive than a non-heme $Cu_2(\mu{-}1,2\text{-}O_2^{\bullet-})$ complex in reaction with N–H bonds. These results add to the growing body of evidence that metal-superoxide species in biologically relevant environments may function as oxidants for certain organic substrates, although the oxidation of C–H bonds remains quite challenging for such species. The factors that control the relative reactivity of $M(O_2^{\bullet-})$ species remain poorly understood, providing motivation for further research in this area. The authors acknowledge research support from the NIH (GM101153 to D. P. G.).

Supplementary Material

Refer to Web version on PubMed Central for supplementary material.

Notes and references

1. Sahu S and Goldberg DP, J Am Chem Soc, 2016, 138, 11410–11428. [PubMed: 27576170]
2. (a) Makino R, Obayashi E, Hori H, Iizuka T, Mashima K, Shiro Y and Ishimura Y, Biochemistry, 2015, 54, 3604–3616; [PubMed: 25996254] (b) Booth ES, Basran J, Lee M, Handa S and Raven EL, J. Biol. Chem, 2015, 290, 30924–30930; [PubMed: 26511316] (c) Lewis-Ballester A, Batabyal D, Egawa T, Lu C, Lin Y, Marti MA, Capece L, Estrin DA and Yeh S-R, Proc. Natl. Acad. Sci. U. S. A, 2009, 106, 17371–17376. [PubMed: 19805032]

3. (a) Stoll S, NejatyJahromy Y, Woodward JJ, Ozarowski A, Marletta MA and Britt RD, J. Am. Chem. Soc, 2010, 132, 11812–11823; [PubMed: 20669954] (b) Huang H, Hah J-M and Silverman RB, J. Am. Chem. Soc, 2001, 123, 2674–2676. [PubMed: 11456942]
4. Tchesnokov EP, Faponle AS, Davies CG, Quesne MG, Turner R, Fellner M, Souness RJ, Wilbanks SM, de Visser SP and Jameson GNL, Chem. Commun, 2016, 52, 8814–8817.
5. Xing G, Diao Y, Hoffart LM, Barr EW, Prabhu KS, Arner RJ, Reddy CC, Krebs C and Bollinger JM, Jr., Proc. Natl. Acad. Sci. U. S. A, 2006, 103, 6130–6135. [PubMed: 16606846]
6. Tamanaha E, Zhang B, Guo Y, Chang W-c., Barr EW, Xing G, St. Clair J, Ye S, Neese F, Bollinger JM, Jr., Krebs C, J. Am. Chem. Soc, 2016, 138, 8862–8874. [PubMed: 27193226]
7. Baglia RA, Zaragoza JP and Goldberg DP, Chem. Rev, 2017, 117, 13320–13352. [PubMed: 28991451]
8. (a) Liu J-G, Ohta T, Yamaguchi S, Ogura T, Sakamoto S, Maeda Y and Naruta Y, Angew. Chem. Intl. Ed, 2009, 48, 9262–9267; (b) Liu J-G, Shimizu Y, Ohta T and Naruta Y, J. Am. Chem. Soc, 2010, 132, 3672–3673; [PubMed: 20196593] (c) Nagaraju P, Ohta T, Liu JG, Ogura T and Naruta Y, Chem Commun, 2016, 52, 7213–7216.
9. (a) Niederhoffer EC, Timmons JH and Martell AE, Chem. Rev, 1984, 84, 137–203;(b) Jones RD, Summerville DA and Fred B, Chem. Rev, 1979, 79, 139–179;(c) Busch DH and Alcock NW, Chem. Rev, 1994, 94, 585–623;(d) Smith TD and Pilbrow JR, Coord. Chem. Rev, 1981, 39, 295–383.
10. Early work on Co-porphyrins suggested their Co(O2-) species could abstract H–atoms from phenols. See Wang X-Y, Motekaitis RJ and Martell AE, Inorg. Chem, 1984, 23, 271–275.
11. Wang CC, Chang HC, Lai YC, Fang H, Li CC, Hsu HK, Li ZY, Lin TS, Kuo TS, Neese F, Ye S, Chiang YW, Tsai ML, Liaw WF and Lee WZ, J. Am. Chem. Soc, 2016, 138, 14186–14189. [PubMed: 27726348]
12. Ramdhanie B, Telser J, Caneschi A, Zakharov LN, Rheingold AL and Goldberg DP, J. Am. Chem. Soc, 2004, 126, 2515–2525. [PubMed: 14982461]
13. Warren JJ, Tronic TA and Mayer JM, Chem. Rev, 2010, 110, 6961–7001. [PubMed: 20925411]
14. Ramdhanie B, Zakharov LN, Rheingold AL and Goldberg DP, Inorg. Chem, 2002, 41, 4105–4107. [PubMed: 12160395]
15. (a) Lee JY, Peterson RL, Ohkubo K, Garcia-Bosch I, Himes RA, Woertink J, Moore CD, Solomon EI, Fukuzumi S and Karlin KD, J. Am. Chem. Soc, 2014, 136, 9925–9937; [PubMed: 24953129] (b) Kindermann N, Gunes CJ, Dechert S and Meyer F, J. Am. Chem. Soc, 2017, 139, 9831–9834; [PubMed: 28691811] (c) Tano T, Okubo Y, Kunishita A, Kubo M, Sugimoto H, Fujieda N, Ogura T and Itoh S, Inorg. Chem, 2013, 52, 10431–10437. [PubMed: 24004030]
16. (a) Cho J, Woo J and Nam W, J. Am. Chem. Soc, 2010, 132, 5958–5959; [PubMed: 20392047] (b) Goo YR, Maity AC, Cho KB, Lee YM, Seo MS, Park YJ, Cho J and Nam W, Inorg. Chem, 2015, 54, 10513–10520; [PubMed: 26486819] (c) Nemes A and Bakac A, Inorg. Chem, 2001, 40, 746–749. [PubMed: 11225118]
17. Company A, Yao S, Ray K and Driess M, Chemistry, 2010, 16, 9669–9675. [PubMed: 20645352]
18. (a) Hong S, Sutherlin KD, Park J, Kwon E, Siegler MA, Solomon EI and Nam W, Nat. Commun, 2014, 5, 5440; [PubMed: 25510711] (b) Chiang CW, Kleespies ST, Stout HD, Meier KK, Li PY, Bominaar EL, Que L, Jr., Munck E and Lee WZ, J. Am. Chem. Soc, 2014, 136, 10846–10849. [PubMed: 25036460]
19. Corona T, Padamati SK, Acuna-Pares F, Duboc C, Browne WR and Company A, Chem. Commun, 2017, 53, 11782–11785.

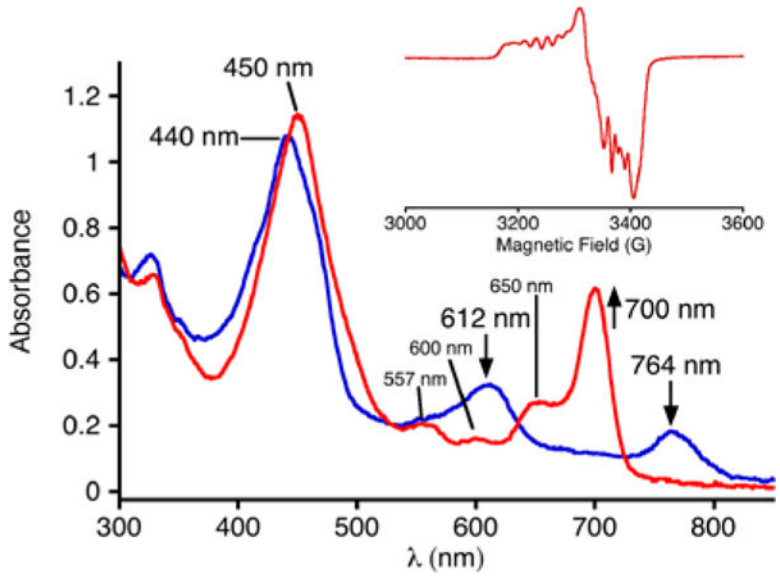

Fig. 1.

UV-vis spectra for $[Co^{II}(py)(TBP_8Cz)]^-$ (blue line) and $[Co^{III}(py)(O_2)(TBP_8Cz)]^-$ (red line), 18 μM in CH_2Cl_2/pyridine (99/1, v/v) at −65 °C. Inset: X-band EPR spectra at 15 K for $[Co^{III}(py)(O_2)(TBP_8Cz)]^-$.

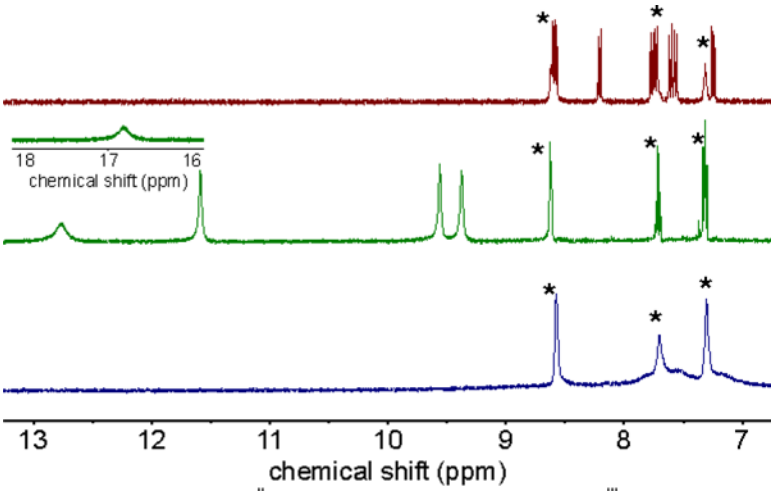

Fig. 2.

^{1}H NMR spectra of $Co^{III}(py)_2(TBP_8Cz)$ (red line) at 25 °C, $[Co^{II}(py)(TBP_8Cz)]^-$ (green line) at 25 °C, and $[Co^{III}(py)(O_2)(TBP_8Cz)]^-$ (blue line) in CD_2Cl_2/pyridine-d_5 (20/1 v/v) at −65 °C, showing the aromatic region. * = pyridine peaks

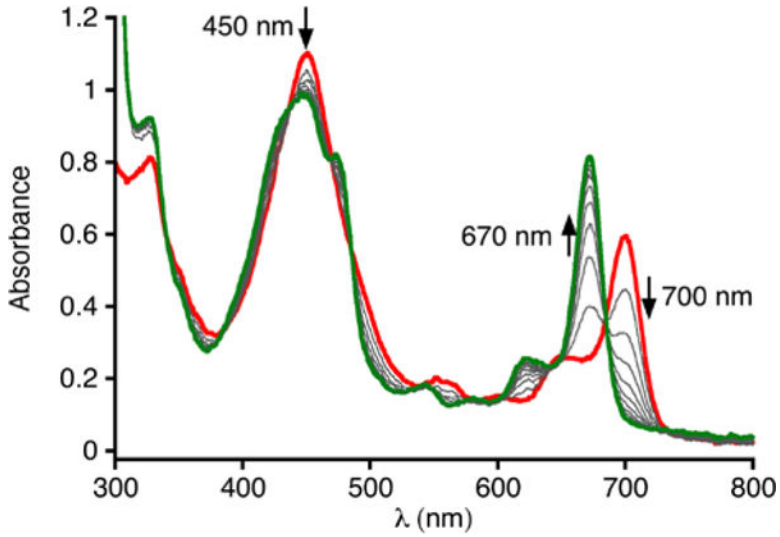

Fig. 3.

Time-resolved UV-vis spectra (0 – 40 min) for the reaction between [Co^{III}(py)(O_2)(TBP_8Cz)]- (18 μM) and DPH (0.33 mM) in CH_2Cl_2/py (99/1, v/v) at −65 °C.

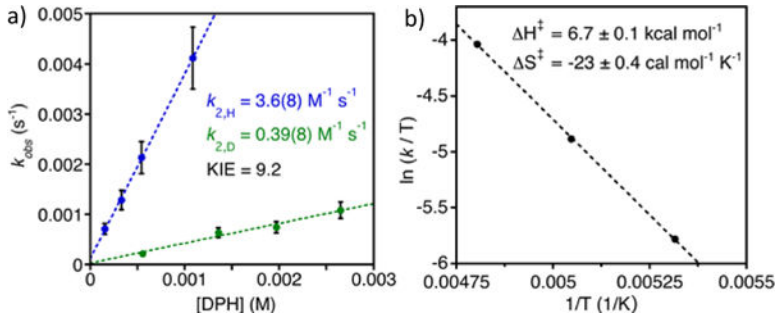

Fig. 4.

(a) Plot of pseudo-first-order rate constants (k_{obs}) versus [DPH] (blue circles) or [DPH-d_2] (green circles) together with best-fit lines. (b) Plot of ln (k/T) versus inverse temperature (Eyring Plot).

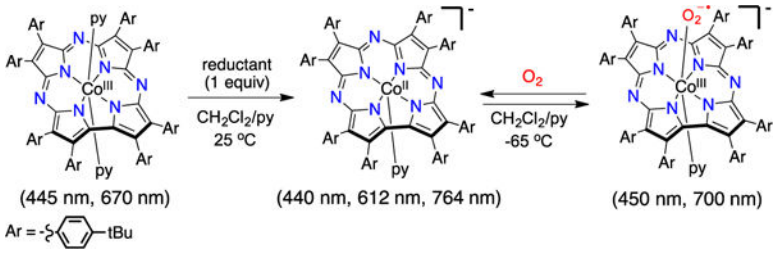

Scheme 1.
Generation of $[Co^{III}(py)(O_2)(TBP_8Cz)]^-$ (**1**)

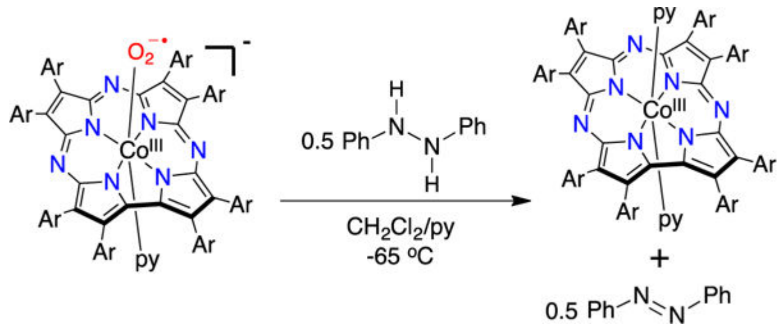

Scheme 2.

Reaction of $[Co^{III}(py)(O_2)(TBP_8Cz)]^{-}$ with the H-atom donor DPH at −65 °C

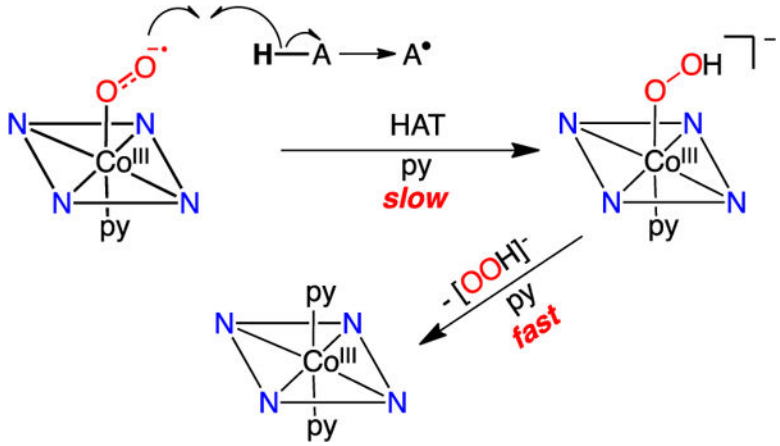

Scheme 3.

Proposed mechanism for the reaction between the cobalt(III)-superoxide complex and H-atom donors.